ASTM INTERNATIONAL

Materials Performance and Characterization

Dumitru Mitrica,[1] Vasile Soare,[2] Ionut Constantin,[2] Marian Burada,[2] Mihai T. Olaru,[2] Viorel Badilita,[3] Victoria Soare,[3] Florentin Stoiciu,[4] Gabriela Popescu,[5] and Ioan Carcea[6]

DOI: 10.1520/MPC20170018

Influence of the Heat Treatment Processes on the Properties of High Entropy Alloys Based on Al-Cr-Fe-Mn-Ni System

Materials Performance and Characterization

doi:10.1520/MPC20170018 available online at www.astm.org

Dumitru Mitrica,[1] Vasile Soare,[2] Ionut Constantin,[2] Marian Burada,[2] Mihai T. Olaru,[2] Viorel Badilita,[3] Victoria Soare,[3] Florentin Stoiciu,[4] Gabriela Popescu,[5] and Ioan Carcea[6]

Influence of the Heat Treatment Processes on the Properties of High Entropy Alloys Based on Al-Cr-Fe-Mn-Ni System

Manuscript received January 26, 2017; accepted for publication May 1, 2017; published online September 19, 2017.

[1] National R&D Institute for Nonferrous and Rare Metals, New Materials and Technologies Laboratory, 102 Biruintei Blvd, 739571 Pantelimon, Romania (Corresponding author), e-mail: dmitrica@imnr.ro, https://orcid.org/0000-0001-8306-9246

[2] National R&D Institute for Nonferrous and Rare Metals, New Materials and Technologies Laboratory, 102 Biruintei Blvd, 739571 Pantelimon, Romania

[3] National R&D Institute for Nonferrous and Rare Metals, Physical and Chemical Laboratory, 102 Biruintei Blvd, 739571 Pantelimon, Romania

[4] National R&D Institute for Nonferrous and Rare Metals, Microscopic Characterization Laboratory, 102 Biruintei Blvd, 739571 Pantelimon, Romania

[5] Polytechnic University of Bucharest, Centre for Research and Expertizing of Special Materials, 313 Splaiul Independentei, sector 6, 060032 Bucharest, Romania

[6] Gheorghe Asachi Technical University of Iasi, Faculty of Materials Science and Engineering, 67 Profesor Dimitrie Mangeron Blvd, 700050 Iasi, Romania

Reference

Mitrica, D., Soare, V., Constantin, I., Burada, M., Olaru, M. T., Badilita, V., Soare, V., Stoiciu, F., Popescu, G., and Carcea, I., "Influence of the Heat Treatment Processes on the Properties of High Entropy Alloys Based on Al-Cr-Fe-Mn-Ni System," *Materials Performance and Characterization* https://doi.org/10.1520/MPC20170018. ISSN 2379-1365

ABSTRACT

In the present paper, high entropy alloys based on an aluminum-chromium-iron-manganese-nickel (Al-Cr-Fe-Mn-Ni) system were prepared by induction melting and annealed in an inert atmosphere. The resulting samples were analyzed by optical microscopy, scanning electron microscopy, and X-ray diffraction to determine the structural characteristics before and after the heat treatment process. Significant phase transformations and changes in the phase distribution were noticed after the heat treatment process. The results were discussed against the thermodynamic criteria calculations for most promising compositions. Hardness tests were provided for the selected samples to indicate the changes in the mechanical properties between various compositions and between as-cast and annealed samples. Results indicated that the heat treatment process determined a significant hardness increase in one of the studied high entropy alloys.

Keywords

high entropy alloy, heat treatment, characterization

Introduction

Newly emerged high entropy alloys (HEAs) are advanced metallic materials that exhibit a wide range of excellent mechanical and physical properties such as high strength and

toughness, high stiffness, and improved corrosion resistance. HEAs are composed of five or more principle elements in equal proportions. While the high strength of conventional metals and alloys rely mostly on the controlled distribution of a second phase, HEA properties are based on solid solution strengthening effects and the suppression of intermetallic phases [1,2]. There is little information in literature regarding phase diagrams for HEAs due to the high number of elements and the difficulty of obtaining thermodynamically stable structures.

Previous research work on HEAs is based on various systems [3–9], among which aluminum-chromium-iron-manganese-nickel (Al-Co-Cr-Fe-Ni) represents the most studied system [10–14]. HEAs are mainly composed of transitional elements and usually form face-centered cubic (FCC) or body-centered cubic (BCC) structures, or a mix of the two [15]. FCC type alloys are softer and ductile, whereas BCC alloys are stronger and brittle. It is known that chromium is a BCC stabilizer [16], whereas nickel is an FCC stabilizer. The equations for the nickel equivalent (N_{eq} = Ni % + 0.5 Mn % + 0.25 Cu %, atomic percentage) as FCC-forming ability and chromium equivalent (Cr_{eq} = Cr % + Fe %, atomic percentage) as BCC-forming ability were developed by Ren et al. [17] and are similar to stainless steels. Furthermore, aluminum has the ability to change the structural behavior of the alloy from FCC to BCC through additions over certain limits. In general, equimolar addition of aluminum will produce dominant BCC phases in HEAs.

The preferential formation of solid solutions and the distinctive sluggish diffusion of HEA structures suggest potential for tailoring the final properties by subsequent and well-controlled heat treatment stages. In general, the final alloy structure has been found to be influenced widely by alloy composition, melting/casting conditions, and heat treatment conditions. Among the few reports found in literature, special attention was dedicated to cobalt-containing HEAs due to their early stage development. Cobalt (an FCC-forming element) in HEAs was found to increase the mechanical resistance of the alloy after annealing at up to 600°C, but a significant drop in hardness is observed after annealing at higher temperatures [18,19]. Recently, Chen et al. [20] found that if cobalt is replaced with manganese, twice the increase in alloy hardness will be registered after annealing at 800°C, especially for alloys with lower aluminum content (containing FCC phases).

The present paper proposes the study of several compositions of HEAs with less critical metal content and the ability to maintain high hardness levels after extended work at high temperatures, making them feasible for fabrication of dies and rolling equipment of high mechanical endurance. A thermodynamic evaluation was also performed for several promising compositions.

Experimental

HEAs $Al_{0.3}Cr_{1.5}Fe_{1.5}MnNi_{0.5}$, $Al_{0.5}Cr_{1.5}Fe_{1.5}MnNi_{0.5}$, and $Al_{0.5}Cr_2Fe_{1.5}MnNi$ were prepared in an induction furnace with inert atmosphere, a Linn MFG–30, and cast in a copper crucible. Technical purity (99.9 %) elementals aluminum, chromium, iron, manganese, and nickel were used as raw materials. A 500-g charge of each alloy composition was initially loaded and melted under argon atmosphere (at 100 kPa) in a zirconia-based crucible. The alloy was remelted to ensure a uniform chemical composition. The resulted as-cast alloys were annealed in an electrical furnace, LHT 04/17 Nabertherm GMBH, with a protective atmosphere (argon gas) and maximum temperature of 1,700°C. The heat treatment stage was conducted at 900°C for 20 h with slow furnace cooling. Samples

were taken before and after the heat treatment process for chemical, structural, and mechanical analyses.

The chemical composition of the alloy was determined by inductively coupled plasma optical emission spectrometry (ICP-OES) using an Agilent 725 spectrometer. The optical microscopy investigation was performed with a Zeiss Axio Scope A1m Imager microscope. Samples were previously etched in an HCl-HNO_3-CH_3COOH-H_2O solution to enhance the visibility of the grains and the grain boundaries. The morphology of the alloy was analyzed by scanning electron microscopy (SEM) using a FEI Quanta 3D FEG operating at 20–30 kV, equipped with an energy dispersive X-ray spectrometer (EDS). The phase structure was analyzed by X-ray diffractometry (XRD). Data acquisition was performed on BRUKER D8 ADVANCE diffractometer, using Bruker®DIFFRAC plus software, Bragg-Brentano diffraction method, Θ - Θ coupled in vertical configuration, with the following parameters: CuKα radiation, 2Θ Region: 20 ÷ 1240, 2Θ Step: 0.020, Time/step: 8.7 s/step. Cukβ radiation was removed with a SOL X detector. The resulting data was processed using Bruker® Diffracplus EVA v12 software to search the database ICDD Powder Diffraction File (PDF-2, 2006 edition) and the Full Pattern Matching (FPM) module of the same software package. Vickers microhardness of the samples was measured at room temperature using an optical microscope attachment (Anton Paar MHT10) with an applied load of 2 N and slope of 0.6 N/s. In order to determine the average hardness of the alloy, seven indentations were made on the surface of the as-cast and re-melted samples.

Results and Discussions

COMPOSITIONAL SCREENING PROCESS

The authors initially selected several alloy systems (AlCrCuFeMnNi, AlCrCoFeNiTi, AlCrCuFeMnNiSi, and AlCrFeMnNi) with low critical and less expensive element content (aluminum, iron, manganese, silicon). The selection process was based mostly on the literature review for certain types of alloys. In order to improve the alloys properties, several elemental additions were performed (manganese, titanium, and silicon) that potentially could improve the properties required by intended application: wear resistance, corrosion resistance, and stability at high temperatures. The experimental results were published previously and showed unsatisfactory results that were caused by interdendritic segregations (copper) [7], brittle structures [21,22], and/or low corrosion resistance [7,21].

The AlCrFeMnNi system proved to offer the most promising solution due to its high potential for tailoring the properties through composition variation and thermomechanical treatment. A selection of viable compositions was performed previously using a guided screening process based on the previous experimental results, showing the influence of certain element addition to the structure and properties of HEA, and based on thermodynamic calculations using the latest knowledge on the theoretical criteria development.

Among the transitional elements, iron and nickel are found in most of the entropy alloys because of their ability to form thermodynamically stable alloys in combination with other elements. Chromium has the role of increasing mechanical strength and corrosion resistance. Manganese replaces cobalt (a critical element) and promotes the formation of complex solid solutions. Aluminum has a hardening role but also the potential for fine adjustment of the mechanical properties of HEA alloys because it has the ability to change the structural behavior of the alloy from FCC to BCC through additions over certain limits.

As the HEAs were defined initially, the mechanism for the formation of simple solid solution phases in HEA relies on the thermodynamic assessment based on Boltzmann's hypothesis, which states that the maximum entropy of mixing an alloy is obtained at equiatomic compositions.

The sufficiency of the above statement was later discussed, and it was found, through experimental and theoretical analyses, that several alloy compositions that met the entropy criterion do not form exclusively solid solution structures. In these cases, high negative values of mixing enthalpy (ΔH_{mix}) plays an important role in diminishing the high entropy effect, and intermetallic secondary phases will form in the final structure.

Additional criteria were introduced [23,24] based on the Hume-Rothery rule of solid solution formation and contain several important conditions on small differences between atomic sizes (δ), electronegativity ($\Delta\chi$), and valence electron concentration (VEC) between elements. Also, an Ω factor was introduced later by Yang and Zhang [25] to better approximate the influence of mixing enthalpy on the formation of solid solution phases.

The criteria parameters are calculated with the following equations:

$$\Delta S_{mix} = -R \cdot \sum c_i \cdot lnc_i \tag{1}$$

$$\Delta H_{mix} = \sum 4c_i c_j \cdot \Delta H_{ij} \tag{2}$$

$$\delta = 100 \cdot \sqrt{\sum c_i \cdot \left(1 - \frac{r_i}{\bar{r}}\right)^2} \tag{3}$$

$$\Delta\chi = 100 \cdot \sqrt{\sum c_i \cdot \left(1 - \frac{\chi_i}{\bar{\chi}}\right)^2} \tag{4}$$

$$VEC = \sum c_i \cdot VEC_i \tag{5}$$

$$\Omega = T_m \Delta S_{mix} / |\Delta H_{mix}| \tag{6}$$

The symbols in the formulas are described as follows: R is gas constant (8.314 J/molK), c_i is the atomic fraction for element i, ΔH_{ij} is the binary enthalpy of mixing for element i and j, r_i is the atomic radius of element i, $\bar{r}$ is the average atomic radius, χ_i is electronegativity of element i, $\bar{\chi}$ is average electronegativity, VEC_i is valence electron concentration of element i, and T_m is the melting temperature calculated with $T_m = \Sigma c_i \cdot T_{mi}$ (where T_{mi} is the melting temperature of element i).

The authors provided certain numerical intervals to distinguish the type of structure for the majority of HEAs. To summarize the results, we present here the most accepted values for the formation of solid solution structures:

- Entropy of mixing (ΔS_{mix}) higher than 11 J/moleK and lower than 19.5 J/moleK.
- Enthalpy of mixing (ΔH_{mix}) between −22 and 7 kJ/mol.
- A small atomic size difference of $\delta < 6.6$ %, for the preponderant formation of solid solutions and $\delta < 4$ % to obtain only solid solutions.
- When parameters $\Omega > 1.1$ and $\delta < 3.6$ % only solid solutions are formed. If $1.1 < \Omega < 10$ and $3.6\ \% < \delta < 6.6$ %, solid solutions and intermetallic compounds are formed, and if $\Omega > 10$, only solid solutions are formed.
- Allen electronegativity difference ($\Delta\chi$) of 3 % to 6 % indicates the presence of only solid solutions.

TABLE 1
Criteria parameters for several Al-Cr-Fe-Mn-Ni system based compositions.

Symbol	Alloy	$\Delta Sconf$, J/molK	$\Delta Hmix$, kJ/mol	δ, %	VEC, %	$\Delta\chi mix$, %	Tm, K	Ω
HEA1	$Al_{0.5}CrFeMnNi$	13.14	−9.28	5.19	7.33	5.39	1,700	2.4
HEA2	$AlCrFeMnNi$	13.38	−12.48	5.82	7	5.6	1,623	1.74
HEA3	$Al_{1.5}CrFeMnNi$	13.25	−14.41	6.3	6.72	5.77	1,560	1.43
HEA4	$Al_{0.5}Cr_{1.5}FeMnNi$	12.94	−8.4	5.1	7.2	5.36	1,742	2.68
HEA5	$Al_{0.5}Cr_{1.5}Fe_{1.5}MnNi$	12.85	−7.53	5.07	7.27	5.22	1,748	2.98
HEA6	$Al_{0.5}Cr_2Fe_{1.5}MnNi$	12.61	−6.97	4.72	7.16	5.21	1,780	3.22
HEA7	$Al_{0.5}Cr_{1.5}Fe_{1.5}MnNi_{0.5}$	12.51	−6.52	5.00	7	4.85	1,751	3.36
HEA8	$Al_{0.5}Cr_{1.5}Fe_{1.5}MnNi_{1.5}$	12.84	−7.53	5.02	7.5	5.53	1,747	2.76
HEA9	$Al_{0.3}CrFe_{1.5}MnNi$	12.61	−6.55	4.86	7.54	5.14	1,743	3.35
HEA10	$Al_{0.3}CrFe_{1.5}MnNi_{0.5}$	12.32	−5.5	4.70	7.26	4.6	1,745	3.9
HEA11	$Al_{0.3}Cr_{1.5}Fe_{1.5}MnNi_{0.5}$	12.17	−4.94	4.53	7.12	4.71	1,785	4.39

- Valence electron concentration determines the type of solid solutions. Only a BCC structure is formed when $VEC \leq 6.87$, BCC and FCC structures for $6.87 \leq VEC \leq 8$, and only FCC for $VEC > 8$

A preliminary group comprising 53 different compositions, based on the Al-Cr-Fe-Mn-Ni system, was selected in the present research, among which 11 have the most practical interest for us because of the influence of component elements: aluminum with high influence over the type of solid solutions (BCC or FCC), iron to lower the alloy price, chromium to raise alloy hardness, and nickel to lower alloy price and decrease potential NiAl-based phases.

The calculation results (Table 1) show that all compositions develop mainly solid solutions, but HEA7 to HEA11 have lower mixing enthalpy and can form intermetallic phases. The atomic size difference of all compositions shows preponderant formation of solid solutions, while Ω factor shows formation of complex solid solution and intermetallic phases, a statement that cannot be verified by the electronegativity criterion. Only one composition ($Al_{1.5}CrFeMnNi$) has VEC lower than 6.87 and should form only BCC phases, while the rest of them should have mixed FCC and BCC phases.

$Al_{0.5}Cr_2Fe_{1.5}MnNi$, $Al_{0.5}Cr_{1.5}Fe_{1.5}MnNi_{0.5}$, and $Al_{0.3}Cr_{1.5}Fe_{1.5}MnNi_{0.5}$ show a higher melting temperature and a structure composed of BCC, FCC, and intermetallic compounds, which is desirable for high temperature stability, high hardness, and fatigue resistance.

CHARACTERISATION RESULTS AND DISCUSSION

The chemical analyses of as-cast samples indicate that the composition was relatively uniform across the ingot section and very close to the nominal values (Table 2).

The results of microstructural analyses (Figs. 1–3) by optical microscopy revealed significantly different morphologies between as-cast and heat-treated states for all alloy compositions. The $Al_{0.3}Cr_{1.5}Fe_{1.5}MnNi_{0.5}$ alloy showed a wide dendritic area (darker region) that contained a fine eutectic-like structure composed of precipitates embedded in a large solid solution structure. In the as-cast structure there were small and rounded phases (light brown color), uniformly dispersed in the alloy mass. The heat-treated alloy shows a highly homogeneous structure composed of a large eutectic-like area and uniformly distributed hard phases of small dimensions. The as-cast $Al_{0.5}Cr_{1.5}Fe_{1.5}MnNi_{0.5}$ and

TABLE 2
The obtained (actual) and calculated (nominal) chemical composition of the studied alloys.

Alloy type	Composition Type	Composition, wt. %				
		Al	Cr	Fe	Mn	Ni
$Al_{0.3}Cr_{1.5}Fe_{1.5}MnNi_{0.5}$	calculated	3.18	30.69	32.96	21.61	11.54
	actual	3.15	30.7	33.6	20.3	12.2
$Al_{0.5}Cr_{1.5}Fe_{1.5}MnNi_{0.5}$	calculated	5.2	30.05	32.28	21.16	11.3
	actual	5.41	28.9	33.4	23.2	12.8
$Al_{0.5}Cr_2Fe_{1.5}MnNi$	nominal	3.82	30.6	27.3	18.2	19.8
	actual	4.3	33.02	26.6	17.44	18.63

FIG. 1 Optical microscopy of $Al_{0.3}Cr_{1.5}Fe_{1.5}MnNi_{0.5}$ alloy before (a) and after (b) heat treatment.

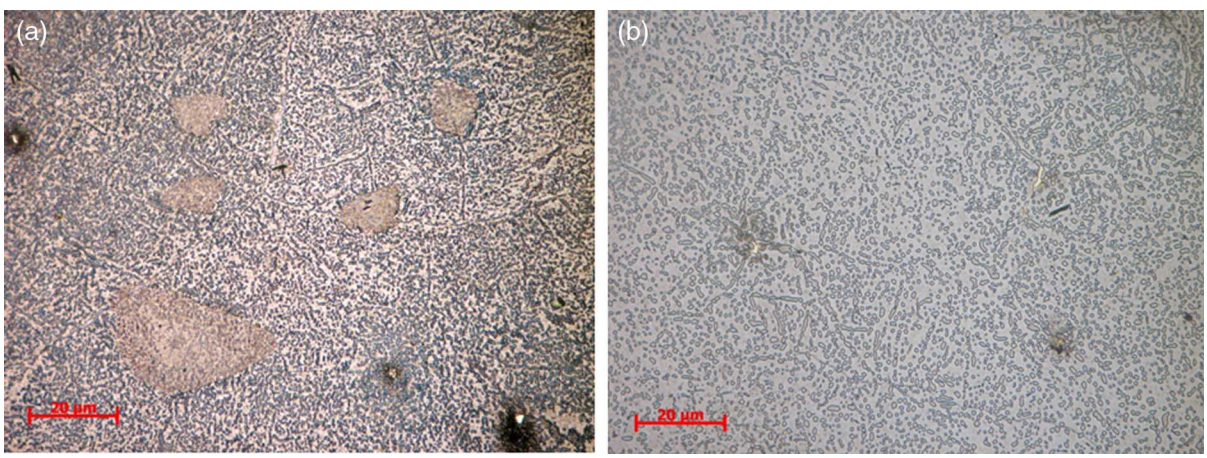

FIG. 2 Optical microscopy of $Al_{0.5}Cr_{1.5}Fe_{1.5}MnNi_{0.5}$ alloy before (a) and after (b) heat treatment.

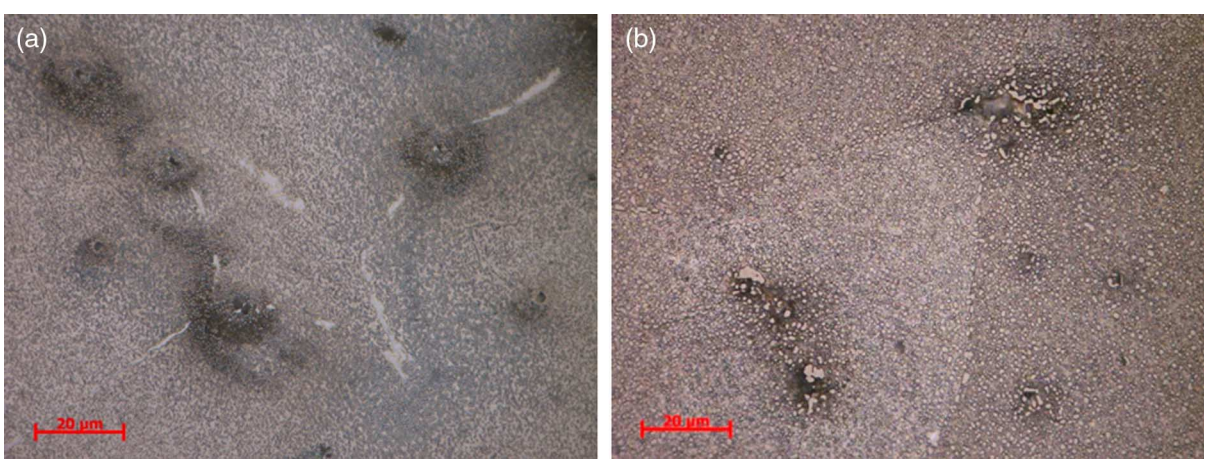

FIG. 3 Optical microscopy of $Al_{0.5}Cr_2Fe_{1.5}MnNi$ alloy before (a) and after (b) heat treatment.

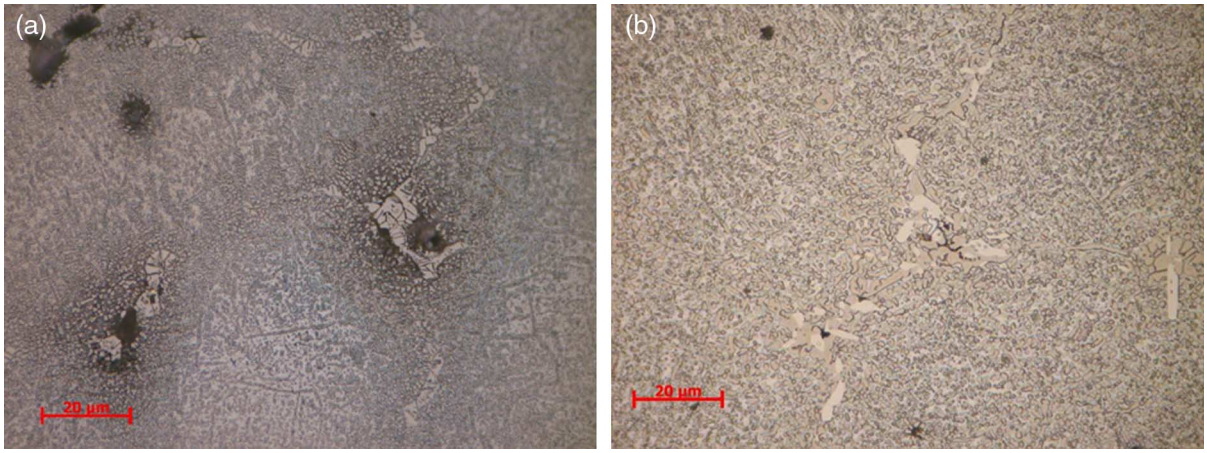

$Al_{0.5}Cr_2Fe_{1.5}MnNi$ alloys had distinguished dendrite formations composed of eutectic-like precipitates, but no rounded phases were observed. Instead, intermetallic formations were found uniformly dispersed in the alloy. The heat-treated microstructures show equiaxed grain structures with well-defined eutectic areas that contained larger precipitates. Segregated phases appear at grain boundaries and cover a larger area in the $Al_{0.5}Cr_2Fe_{1.5}MnNi$ alloy. This shows that the increase of chromium content in the alloy leads to the formation of segregations at grain boundaries, which may cause cracks during the mechanical stresses.

Microstructural analyses at higher magnification levels through SEM show a significant increase in the size of the eutectic precipitates after the heat treatment process in all three alloy compositions (Figs. 4–6). Also, segregations at grain boundaries and significant larger eutectic precipitates are observed in the $Al_{0.5}Cr_2Fe_{1.5}MnNi$ alloy (Fig. 6b). The Energy Dispersive X-ray Analysis (EDAX) mapping (Fig. 7) of a representative area of

FIG. 4 SEM images of $Al_{0.3}Cr_{1.5}Fe_{1.5}MnNi_{0.5}$ alloy before (a) and after (b) heat treatment.

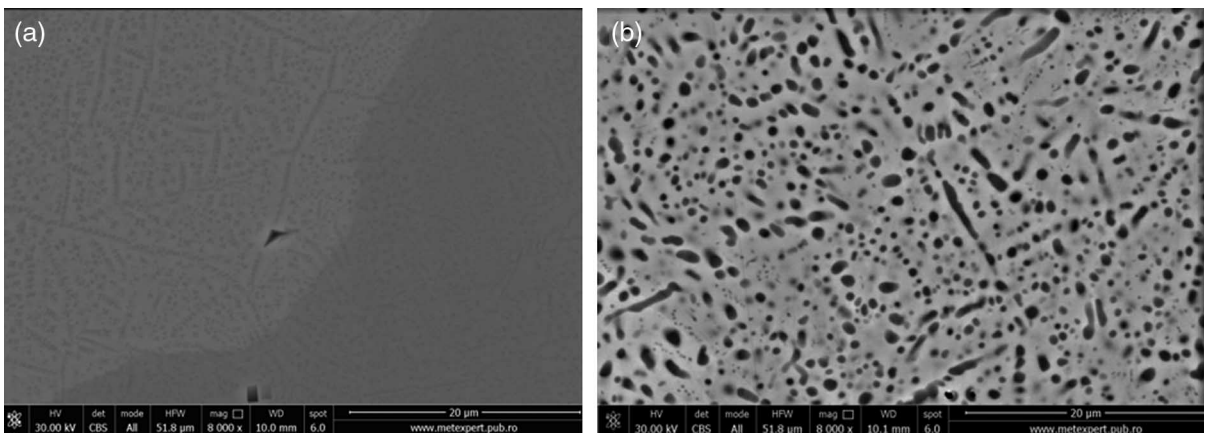

FIG. 5 SEM images of $Al_{0.5}Cr_{1.5}Fe_{1.5}MnNi_{0.5}$ alloy before (a) and after (b) heat treatment.

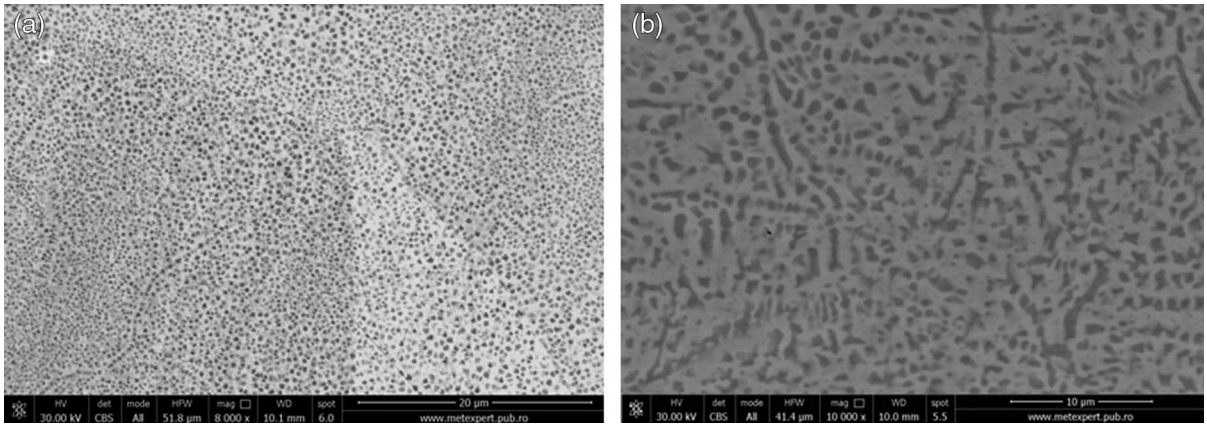

$Al_{0.5}Cr_2Fe_{1.5}MnNi$ alloy structure reveals a high level of iron and nickel segregations in the intergranular area. Aluminum and chromium are found in high concentrations in the grain area where dispersed iron is also present. Nickel is found concentrated in the intergranular area, and manganese is found to have a relatively uniform distribution across the whole structure.

X-ray analyses of the alloy's structure shows significant phase changes between the as-cast and heat-treated states (Table 3). The large difference between phases is also influenced by the high solidification rate of the as-cast alloy (copper mould casting), where non-equilibrium structures can be obtained. The as-cast $Al_{0.3}Cr_{1.5}Fe_{1.5}MnNi_{0.5}$ alloy (Fig. 8) contains a predominant BCC phase (A2 type) and lower content of tetragonal σ phase (FeCr type), while after heat treatment, σ phase becomes dominant and a new FCC phase (A1 type) is formed. The $Al_{0.5}Cr_{1.5}Fe_{1.5}MnNi_{0.5}$ alloy (Fig. 9) contains only BCC phases (A2 and B2 types) in their as-cast states, which are preserved in heat-treated state together with a very low amount of newly formed σ phase. The $Al_{0.5}Cr_2Fe_{1.5}MnNi$ (Fig. 10) alloy contains BCC (A2 and B2 types) and FCC (A1 type)

FIG. 6 SEM images of $Al_{0.5}Cr_2Fe_{1.5}MnNi$ alloy before (a) and after (b) heat treatment.

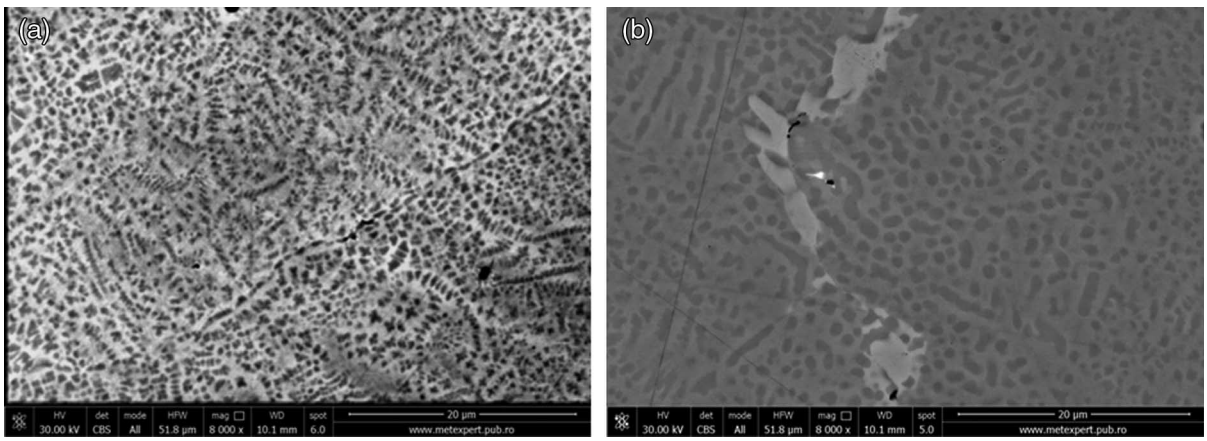

FIG. 7 EDAX analyses of heat-treated $Al_{0.5}Cr_2Fe_{1.5}MnNi$ alloy.

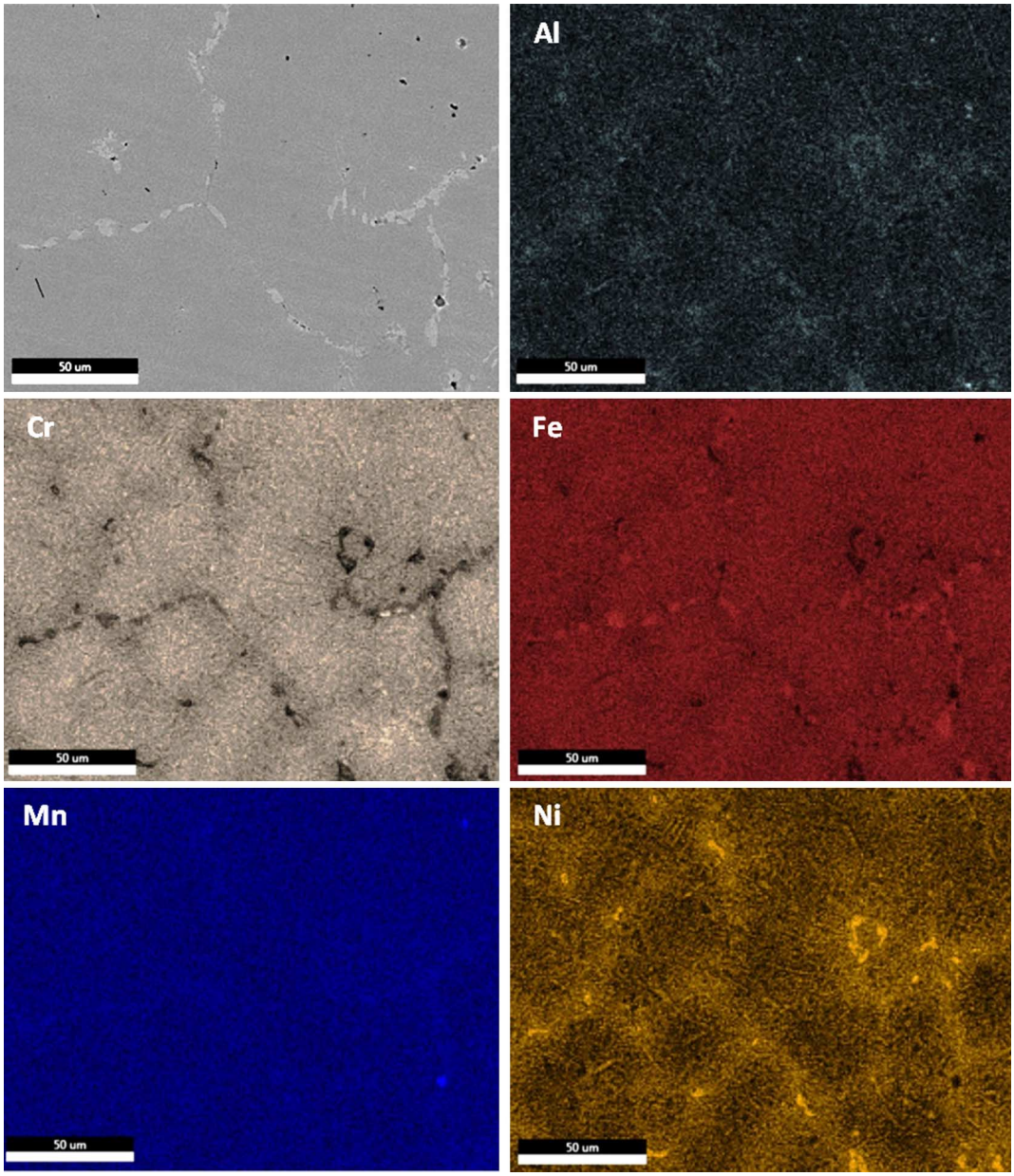

phases in the as-cast state. After the heat treatment process, the FCC phase becomes preponderant in the structure, which also contains the remaining BCC phase (A2 type).

The experimental results showed significant differences compared with the theoretical predictions made previously through criteria calculations, especially for the as-cast specimens. The $Al_{0.3}Cr_{1.5}Fe_{1.5}MnNi_{0.5}$ alloy has no FCC phase in the as-cast state, but it does have all predicted phases in the heat-treated phase. Still, the intermetallic phase is predominant in the heat-treated state. The $Al_{0.5}Cr_{1.5}Fe_{1.5}MnNi_{0.5}$ alloy has no

TABLE 3
Phase evolution after heat treatment.

Alloy Type	Alloy State	Phases
$Al_{0.3}Cr_{1.5}Fe_{1.5}MnNi_{0.5}$	as-cast	A2 type (BCC)
		<20 % σ phase type
	annealed at 900°C	>60 % σ phase type
		A1 type (FCC)
		A2 type (BCC)
$Al_{0.5}Cr_{1.5}Fe_{1.5}MnNi_{0.5}$	as-cast	A2 type (BCC)
		B2 type (BCC)
	annealed at 900°C	A2 type (BCC)
		B2 type (BCC)
		<5% σ phase type
$Al_{0.5}Cr_2Fe_{1.5}MnNi$	as-cast	A2 type (BCC)
		B2 type (BCC)
		>30% A1 type (FCC)
	annealed at 900°C	>60% A1 type (FCC)
		A2 type (BCC)

intermetallic phase present in the as-cast state and no FCC phase in the heat-treated state. The $Al_{0.5}Cr_2Fe_{1.5}MnNi$ alloy has no intermetallic phase in either the as-cast or heat-treated state. However, further research can be performed by annealing the alloys at lower temperatures for a longer period of time in order to reach a completely stable structure.

A different criteria for determining the presence of intermetallic phases in HEAs was provided recently by Senkov and Miracle [26] based on the database provided by Troparevsky et al. [27]. The authors formulated a k_1^{cr} factor based on annealing temperature, mixing entropy, and mixing enthalpy, which needs to be higher than the ratio between intermetallic and mixing enthalpies to form only solid solutions, as expressed in the following equation:

$$k_1^{cr} \equiv 1 - \frac{T_A \Delta S_{mix}}{\Delta H_{mix}}(1 - k_2) > \frac{\Delta H_{IM}}{\Delta H_{mix}} \tag{7}$$

FIG. 8 X-ray diffraction of as-cast (a) and heat-treated (b) $Al_{0.3}Cr_{1.5}Fe_{1.5}MnNi_{0.5}$ alloy.

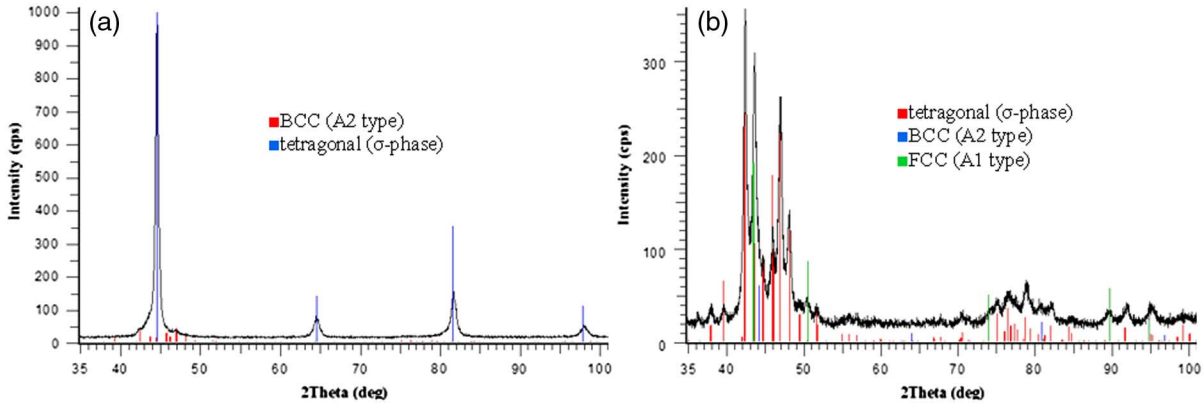

FIG. 9 X-ray diffraction of as-cast (a) and heat-treated (b) $Al_{0.5}Cr_{1.5}Fe_{1.5}MnNi_{0.5}$ alloy.

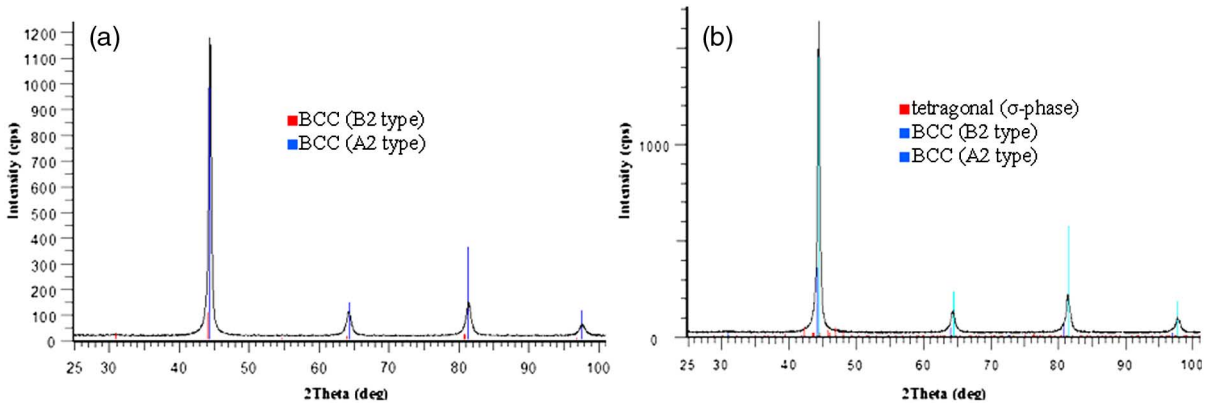

FIG. 10 X-ray diffraction of as-cast (a) and heat-treated (b) $Al_{0.5}Cr_2Fe_{1.5}MnNi$ alloy.

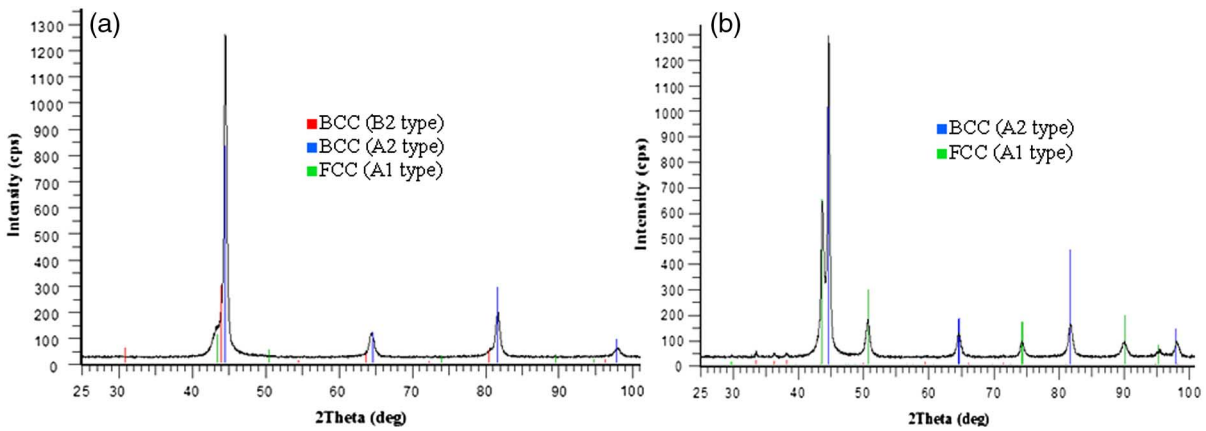

where T_A is the annealing temperature of the alloy, ΔH_{IM} is the enthalpy for formation of intermetallic compounds, and k_2 is a coefficient representing the intermetallic phase entropy over solid solution entropy of mixing and is considered equal with 0.6 for a partially ordered condition. The parameter Ω is calculated now as a function of T_A temperature. Considering $T_A = 1{,}173$ K, the calculations for these criteria (Table 4) show that all alloys have k_1^{cr} smaller than the enthalpy ratio; thus, intermetallic phases may appear in the annealed alloys. The experimental results for $Al_{0.5}Cr_2Fe_{1.5}MnNi$ alloy (no intermetallic phases) show that this criterion is also not entirely verified.

In order to show the potential of studied alloy compositions for application in the tool industry, hardness tests were provided. Vickers microhardness results are presented in Table 5.

The $Al_{0.3}Cr_{1.5}Fe_{1.5}MnNi_{0.5}$ alloy shows a major increase of hardness in its heat-treated state, while the $Al_{0.5}Cr_{1.5}Fe_{1.5}MnNi_{0.5}$ and $Al_{0.5}Cr_2Fe_{1.5}MnNi$ alloys have small changes in hardness values. The correlation of hardness tests and alloy phase composition

TABLE 4
Criteria parameters of selected HEAs in annealed state.

Alloy	ΔH_{IM}	$\Omega(1173)$	k_1^{cr}	$\frac{\Delta H_{IM}}{\Delta H_{mix}}$
$Al_{0.3}Cr_{1.5}Fe_{1.5}MnNi_{0.5}$	−12.76	2.88	2.15	2.58
$Al_{0.5}Cr_{1.5}Fe_{1.5}MnNi_{0.5}$	−16.17	2.25	1.9	2.48
$Al_{0.5}Cr_2Fe_{1.5}MnNi$	−16.03	2.12	1.84	2.3

TABLE 5
Microhardness results.

Alloy type	$Al_{0.3}Cr_{1.5}Fe_{1.5}MnNi_{0.5}$		$Al_{0.5}Cr_{1.5}Fe_{1.5}MnNi_{0.5}$		$Al_{0.5}Cr_2Fe_{1.5}MnNi$	
State	as-cast	annealed	as-cast	annealed	as-cast	annealed
Hardness, HV	424	1,224	481	386	498	440

shows that the high content of hard σ phase in the heat-treated $Al_{0.3}Cr_{1.5}Fe_{1.5}MnNi_{0.5}$ alloy determined a much improved mechanical resistance. Even if the aluminum and chromium content increase in conventional alloys are generally known to strengthen the material, in $Al_{0.5}Cr_{1.5}Fe_{1.5}MnNi_{0.5}$ and $Al_{0.5}Cr_2Fe_{1.5}MnNi$ alloys they determine elemental segregations at grain boundaries, which are detrimental for the alloys' mechanical resistance.

Conclusions

- A selection of the most appropriate compositions of the Al-Cr-Fe-Mn-Ni system was performed based on literature data, known influence of certain elements, and thermodynamic evaluation. Eleven compositions presented interest, among which three were selected for further experimental analyses.
- Three HEAs ($Al_{0.3}Cr_{1.5}Fe_{1.5}MnNi_{0.5}$, $Al_{0.5}Cr_{1.5}Fe_{1.5}MnNi_{0.5}$, and $Al_{0.5}Cr_2Fe_{1.5}MnNi$) were prepared by induction melting and heat treated at 900°C for 20 h.
- The microstructural characterization revealed a large eutectic-like area containing fine precipitates that increase in size after the heat treatment process. Intergranular elemental segregations is found in the alloys with higher chromium and nickel content. Significant changes in phase constitution were recorded after the annealing process. A high σ phase content was found in the heat-treated $Al_{0.3}Cr_{1.5}Fe_{1.5}MnNi_{0.5}$ alloy.
- The phase constitution in as-cast or heat-treated alloys did not match completely with the thermodynamic criteria predictions. A recently developed criterion for annealed alloys was partially verified experimentally.
- For the alloys with higher aluminum, chromium, and nickel content, Vickers microhardness analyses showed similar values between as-cast and annealed states. The $Al_{0.3}Cr_{1.5}Fe_{1.5}MnNi_{0.5}$ alloy increased its hardness from 424 HV to 1,224 HV after the heat treatment process.

ACKNOWLEDGMENTS

This paper was achieved with the financial support of MEN- UEFISCDI Romania, through Joint Applied Research Project PN-II 270/2014, and with the financial support of ANCSI through the CORE Funding Program, project nr.16200304.

References

[1] Yeh, J. W., "Recent Progress in High-Entropy Alloys," *Annales de Chimie - Science des Matériaux*, Vol. 31, No. 6, 2006, pp. 633–648, https://doi.org/10.3166/acsm.31.633-648

[2] Yeh, J. W. 2002. High entropy multielement alloys. U.S. Patent 20, 020, 159, 914, filed April 29, 2002, and published October 31, 2002, https://www.google.com/patents/US20020159914

[3] Tang, W. Y. and Yeh, J. W., "Effect of Aluminum Content on Plasma Nitrided AlxCoCrCuFeNi High-Entropy Alloys," *Metall. Mater. Trans. A.*, Vol. 40, No. 6, 2009, pp. 1479–1486, https://doi.org/10.1007/s11661-009-9821-5

[4] Varalakshmi, S., Kamaraj, M., and Murty, B. S., "Formation and Stability of Equiatomic and Nonequiatomic Nanocrystalline CuNiCoZnAlTi High-Entropy Alloys by Mechanical Alloying," *Metall. Mater. Trans. A.*, Vol. 41, No. 10, 2010, pp. 2703–2709, https://doi.org/10.1007/s11661-010-0344-x

[5] Senkov, O. N., Wilks, G. B., Scott, J. M., and Miracle, D. B., "Mechanical Properties of Nb25Mo25Ta25W25 and V20Nb20Mo20Ta20W20 Refractory High Entropy Alloys," *Intermet.*, Vol. 19, No. 5, 2011, pp. 698–706, https://doi.org/10.1016/j.intermet.2011.01.004

[6] Zhang, H., Pan, Y., and He, Y. Z., "Synthesis and Characterization of FeCoNiCrCu High-Entropy Alloy Coating by Laser Cladding," *Mater. Des.*, Vol. 32, No. 4, 2011, pp. 1910–1915, https://doi.org/10.1016/j.matdes.2010.12.001

[7] Soare, V., Mitrica, D., Constantin, I., Popescu, G., Csaki, I., Tarcolea, M., and Carcea, I., "The Mechanical and Corrosion Behaviors of As-Cast and Re-Melted AlCrCuFeMnNi Multi-Component High-Entropy Alloy," *Metall. Mater. Trans. A.*, Vol. 46, No. 4, 2015, pp. 1468–1473, https://doi.org/10.1007/s11661-014-2523-7

[8] Mishra, A. K., Samal, S., and Biswas, K., "Solidification Behaviour of Ti-Cu-Fe-Co-Ni High Entropy Alloys," *Trans. Indian Instit. Met.*, Vol. 65, No. 6, 2012, pp. 725–730, https://doi.org/10.1007/s12666-012-0206-x

[9] Mridha, S., Samal, S., Khan, P. Y., Biswas, K., and Govind, K. B., "Processing and Consolidation of Nanocrystalline Cu-Zn-Ti-Fe-Cr High-Entropy Alloys via Mechanical Alloying," *Metall. Mater. Trans. A.*, Vol. 44, No. 10, 2013, pp. 4532–4541, https://doi.org/10.1007/s11661-013-1824-6

[10] Ghassemali, E., Sonkusare, R., Biswas, K., and Gurao, N. P., "In-Situ Study of Crack Initiation and Propagation in a Dual Phase AlCoCrFeNi High Entropy Alloy," *J. Alloys Comp.*, Vol. 710, 2017, pp. 539–546, https://doi.org/10.1016/j.jallcom.2017.03.307

[11] Tung, C. C., Yeh, J. W., Shun, T., Chen, S. K., Huang, Y. S., and Chen, H. C., "On the Elemental Effect of AlCoCrCuFeNi High-Entropy Alloy System," *Mater. Lett.*, Vol. 61, No. 1, 2007, pp. 1–5, https://doi.org/10.1016/j.matlet.2006.03.140

[12] Kao, Y. F., Chen, S. K., Chen, T. J., Chua, P. C., Yeh, J. W., and Lin, S. J., "Electrical, Magnetic, and Hall Properties of AlxCoCrFeNi High-Entropy Alloys," *J. Alloys Comp.*, Vol. 509, No. 5, 2011, pp. 1607–1614, https://doi.org/10.1016/j.jallcom.2010.10.210

[13] Wang, Y. P., Li, B. S., Ren, M. X., Yang, C., and Fu, H. Z., "Microstructure and Compressive Properties of AlCrFeCoNi High Entropy Alloy," *Mater. Sci. Eng. A.*, Vol. 491, Nos. 1-2, 2008, pp. 154–158, https://doi.org/10.1016/j.msea.2008.01.064

[14] Wen, L. H., Kou, H. C., Li, J. S., Chang, H., Xue, X. Y., and Zhou, L., "Effect of Aging Temperature on Microstructure and Properties of AlCoCrCuFeNi High-Entropy Alloy," *Intermet.*, Vol. 17, No. 4, 2009, pp. 266–269, https://doi.org/10.1016/j.intermet.2008.08.012

[15] Zhang, T., Zuo, T., Tang, Z., Gao, M. C., Dahmen, K. A., Liaw, P. K., and Lu, Z. P., "Microstructures and Properties of High-Entropy Alloys," *Prog. Mater. Sci.*, Vol. 61, 2014, pp. 1–93, https://doi.org/10.1016/j.pmatsci.2013.10.001

[16] Chen, G., Ke, G., Hsu, T., and Yeh, J., "FCC and BCC Equivalents in As-Cast Solid Solutions of AlxCoyCrzCu$_{0.5}$FevNiw High-Entropy Alloys," *Annales de*

Chimie - Science des Matériaux, Vol. 31, No. 6, 2006, pp. 669–683, https://doi.org/10.3166/acsm.31.669-684

[17] Ren, B., Liu, Z. X., Li, D. M., Shi, L., Cai, B., and Wang, M. X., "Effect of Elemental Interaction on Microstructure of CuCrFeNiMn High Entropy Alloy System," *J. Alloys Comp.*, Vol. 493, Nos. 1-2, 2010, pp. 148–153, https://doi.org/10.1016/j.jallcom.2009.12.183

[18] Sheng, H. F., Gong, M., and Peng, L. M., "Microstructural Characterization and Mechanical Properties of an $Al_{0.5}$CoCrFeCuNi High-Entropy Alloy in As-Cast and Heat-Treated/Quenched," *Mater. Sci. Eng. A.*, Vol. 567, 2013, pp. 14–20, https://doi.org/10.1016/j.msea.2013.01.006

[19] Schuh, B., Mendez-Martin, F., Völker, B., George, E. P., Clemens, H., Pippan, R., and Hohenwarter, A., "Mechanical Properties, Microstructure and Thermal Stability of a Nanocrystalline CoCrFeMnNi High-Entropy Alloy after Severe Plastic Deformation," *Acta Materialia*, Vol. 96, 2015, pp. 258–268, https://doi.org/10.1016/j.actamat.2015.06.025

[20] Chen, S. T., Tang, W. Y., Kuo, Y. F., Chen, S. Y., Tsau, C. H., Shun, T. T., and Yeh, J. W., "Microstructure and Properties of Age-Hardenable $Al_xCrFe_{1.5}MnNi_{0.5}$ Alloys," *Mater. Sci. Eng. A.*, Vol. 527, Nos. 21-22, 2010, pp. 5818–5825, https://doi.org/10.1016/j.msea.2010.05.052

[21] Soare, V., Mitrica, D., Constantin, I., Badilita, V., Stoiciu, F., Popescu, A. M. J., and Carcea, I., "Influence of the Re-Melting on the Microstructure, Hardness and Corrosion Behaviour of the AlCoCrFeNiTi High-Entropy Alloy," *Mater. Sci. Technol.*, Vol. 31, No. 10, 2015, pp. 1194–1200, https://doi.org/10.1179/1743284715Y.0000000029

[22] Buluc, G., Florea, I., Chelariu, R., Popescu, G., and Carcea, I., "Investigation of the Mechanical Properties of FeNiCrMnSi High Entropy Alloy Wear Resistance," *IOP Conf. Ser.: Mater. Sci. Eng.*, Vol. 133, 2016, https://doi.org/10.1088/1757-899X/133/1/012006

[23] Zhang, Y., Zhou, Y. J., Lin, J. P., Chen, G. L., and Liaw, P. K., "Solid-Solution Phase Formation Rules for Multi-Component Alloys," *Adv. Eng. Mater.*, Vol. 10, No. 6, 2008, pp. 534–538.

[24] Guo, S. and Liu, C. T., "Phase Stability in High Entropy Alloys: Formation of Solid-Solution Phase or Amorphous Phase," *Prog. Nat. Sci: Mater. Int.*, Vol. 21, No. 6, 2011, pp. 433–446, https://doi.org/10.1016/S1002-0071(12)60080-X

[25] Yang, X. and Zhang, Y., "Prediction of High-Entropy Stabilized Solid-Solution in Multi-Component Alloys," *Mater. Chem. Phys.*, Vol. 132, Nos. 2-3, 2012, pp. 233–238, https://doi.org/10.1016/j.matchemphys.2011.11.021

[26] Senkov, O. N. and Miracle, D. B., "A New Thermodynamic Parameter to Predict Formation of Solid Solution or Intermetallic Phases in High Entropy Alloys," *J. Alloys Comp.*, Vol. 658, 2016, pp. 603–607, https://doi.org/10.1016/j.jallcom.2015.10.279

[27] Troparevsky, M. C., Morris, J. R., Kent, P. R. C., Lupini, A. R., and Stocks, G. M., "Criteria for Predicting the Formation of Single-Phase High-Entropy Alloys," *Phys. Rev. X.*, Vol. 5, 2015, Vols. 1-6, https://doi.org/ 10.1103/PhysRevX.5.011041